Biosensors and Bioelectronics 52 (2014) 180–187

Contents lists available at ScienceDirect

Biosensors and Bioelectronics

journal homepage: www.elsevier.com/locate/bios

A paper-based microfluidic electrochemical immunodevice integrated with amplification-by-polymerization for the ultrasensitive multiplexed detection of cancer biomarkers

Yafeng Wu [a], Peng Xue [a], Kam M. Hui [b,c,d,e,*], Yuejun Kang [a,**]

[a] School of Chemical and Biomedical Engineering, Nanyang Technological University, 62 Nanyang Drive, Singapore 637459, Singapore
[b] Division of Cellular and Molecular Research, National Cancer Center, 11 Hospital Drive, Singapore 169610, Singapore
[c] Department of Biochemistry, Yong Loo Lin School of Medicine, National University of Singapore, Singapore
[d] Institute of Molecular and Cell Biology, A*STAR, Biopolis Drive Proteos, Singapore
[e] Program in Cancer and Stem Cell Biology, Duke-NUS Graduate Medical School, Singapore

ARTICLE INFO

Article history:
Received 16 June 2013
Received in revised form
20 August 2013
Accepted 20 August 2013
Available online 31 August 2013

Keywords:
Paper-based microfluidic electrochemical immunodevice
Immunoassay
Amplification-by-polymerization
Multiplexed measurement of cancer biomarkers

ABSTRACT

A novel signal amplification strategy for ultrasensitive multiplexed detection of cancer biomarkers using a paper-based microfluidic electrochemical immunodevice is described. Specifically, a controlled radical polymerization reaction is triggered after the capture of target molecules on the immunodevice surface. Growth of long chain polymeric materials provides numerous sites for subsequent horseradish peroxidase (HRP) coupling, which in turn significantly enhances electrochemical signal output. The signal was further amplified through the use of graphene to modify the immunodevice surface to accelerate the electron transfer. Activators generated electron transfer for atom transfer radical polymerization (AGET ATRP) was used in this study for its high efficiency in polymer grafting and better tolerance toward oxygen in air. Glycidyl methacrylate (GMA) was examined to provide excess epoxy groups for HRP coupling. In the electrochemical immunodevice, eight carbon working electrodes, as well as their conductive pads, were screen-printed on a piece of square paper, and the same Ag/AgCl reference and carbon counter electrodes were shared with another piece of square paper via stacking. Using the HRP-*O*-phenylenediamine-H_2O_2 electrochemical detection system, four cancer biomarkers: carcinoembryonic antigen (CEA), alpha-fetoprotein (AFP), cancer antigen 125 (CA125), and carbohydrate antigen 153 (CA153) were detected. A limit of detection of 0.01, 0.01, 0.05 and 0.05 ng mL^{-1} was demonstrated, respectively. The results show that the proposed strategy offers great promises in providing a sensitive and cost-effective solution for biosensing applications.

1. Introduction

Multiplexed immunoassay of biomarkers has recently attracted considerable interest due to its advantages in early screening of diseases, evaluating the extent of diseases, and monitoring the response of diseases to therapy (Geissler et al., 2012). Whitesides and coworkers introduced a promising concept of using patterned paper substrate as microfluidic platform for multiplex analyte detection (Martinez et al., 2007, 2008). Microfluidic paper-based analytical devices (μPADs) have gained more and more attention and great interest during the recent years (Schilling et al., 2012; Martinez et al., 2010; Sia and Kricka, 2008a; Mentele et al., 2012; Wang et al., 2013). It is a promising technology for point-of-care testing (POCT), public health and environmental monitoring applications, in which highly sensitive methods and complex function must be combined with low-cost, rapid and simple fabrication and operation (Sia and Kricka, 2008b; Whitesides, 2011).

To date, many methods have been developed for qualitative and quantitative analyses of multiplex analytes on μPADs, such as colorimetric method (Olkkonen et al., 2010; Abe et al., 2008; Bruzewicz et al., 2008; Lu et al., 2009; Noh and Phillips, 2010; Cheng et al., 2010; Apilux et al., 2010), electrochemical method (Wang et al., 2012a), chemiluminescent method (Yu et al., 2011) and electrochemiluminescent method (Ge et al., 2012b). Some of the methods not only retain the features of simplicity, low cost, portability and disposability of paper-based analytical devices, but also provide new opportunities and directions in the development of precise and sensitive diagnostic devices. Nevertheless, the increasing demand for screening diseases at their early stage of development calls for ultrasensitive detection of biologically

* Corresponding author at: Division of Cellular and Molecular Research, National Cancer Center, 11 Hospital Drive, Singapore 169610, Singapore.
** Corresponding author. Tel.: +65 6316 2894; fax: +65 6791 1761.
E-mail addresses: cmrhkm@nccs.com.sg (K.M. Hui), yuejun.kang@ntu.edu.sg (Y. Kang).

0956-5663/$ - see front matter © 2013 Elsevier B.V. All rights reserved.
http://dx.doi.org/10.1016/j.bios.2013.08.039

relevant molecules at an extremely low level of expression, which inevitably leads to intense research efforts toward exploring novel means to enhance detection sensitivity. Some successful strategies include the employment of new redox-active probes, the integration of enzyme-assisted signal amplification processes, and the incorporation of nanomaterials to increase the upload of signal tags, etc (Karra et al., 2013; Fu et al., 2013; Xu et al., 2013; Coll et al., 2013; Lei and Ju, 2012). The last approach is particularly effective by introducing multiple signal tags per binding event. Similar to nanoparticles, long chain polymeric materials with numerous chemically modifiable functional groups are capable of providing extra signal tags in the same fashion. Indeed, the use of polymer films to increase the loading of signal tags has been routinely employed (Wu et al., 2009, 2010, 2011).

In this report, we described coupling of polymerization-assisted signal amplification with paper-based microfluidic electrochemical immunodevice for multiplexed detection of cancer biomarkers, in an attempt to further enhance sensing sensitivity as well as to provide an interface compatible to existing commercial sensing techniques based on electrochemical readouts. Paper-based microfluidic electrochemical immunodevice (Scheme 1A) was prepared based on the photoresist-patterning technique and screen-printed paper-electrodes. AGET ATRP was used in polymerization for its tolerance to oxygen in the air. Glycidyl methacrylate (GMA) was used as the monomers to provide epoxy groups for immobilization of electrochemical tags (HRP). Four cancer biomarkers, namely, carcinoembryonic antigen (CEA), alpha-fetoprotein (AFP), cancer antigen 125 (CA125), and carbohydrate antigen 153 (CA153), were used as model analytes. These biomarkers were detected using the HRP-*O*-phenylenediamine-H_2O_2 electrochemical system under optimized conditions. This method showed the effectiveness of the proposed strategies of signal amplification for the ultrasensitive detection of cancer biomarkers.

2. Experimental section

2.1. Materials and reagents

Human CEA, AFP, CA125, and CA153 standard solutions, mouse monoclonal capture and signal CEA, AFP, CA125, and CA153 antibodies, and HRP-labeled signal CEA, AFP, CA125, and CA153 antibodies were purchased from Meridian Life Science Inc. (TN, USA). 1-Ethyl-3-(3-dimethylaminopropyl) carbodiimide hydrochloride (EDC), *N*-hydroxysuccinimide (NHS), ascorbic acid, 2,2′-bipyridyl (bpy), $CuCl_2$, *N*,*N*-dimethylformamide (DMF), Tween-20, HRP, glutaraldehyde (25% aqueous solution), chitosan, bovine serum albumin (BSA), *O*-phenylenediamine, and H_2O_2 were obtained from Sigma-Aldrich (MO, USA). Glycidyl methacrylate (GMA) was obtained from Alfa Aesar (Ward Hill, MA) and purified in house to remove the inhibitor (Lou and He, 2006; Qian and He, 2009a, 2009b). A negative photoresist SU-8 3010 and developer were purchased from MicroChem Corp. (Newton, MA, USA). Carbon ink (ELECTRODEDAGPF-407C) and silver/silver chloride ink (ELECTRODAG7019 (18DB19C)) were purchased from Acheson (Germany). Whatman chromatography paper #1 (200.0 mm × 200.0 mm, pure cellulose paper) was obtained from GE Healthcare Worldwide (Pudong Shanghai, China) and used with further adjustment of the paper size. All other chemicals were of analytical grade and were used as received. Twice-distilled water was used throughout the study.

2.2. Apparatus

Differential pulse voltammetric (DPV) measurements and electrochemical impedance spectroscopy (EIS) were performed with a CHI 660C electrochemical workstation (CH Instrument Co., Shanghai, China). Scanning electron microscopic (SEM) images were obtained using a JEOL JSM-5510 scanning electron microscope (Japan). The UV–vis absorption spectra were recorded with a UV-3600 UV–vis-near-infrared (NIR) spectrophotometer (Shimadzu, Japan).

2.3. Fabrication of paper-based microfluidic electrochemical immunodevice

The paper-based microfluidic electrochemical immunodevice consists of two layers of selectively patterned square filter paper of the same size (35.0 mm × 35.0 mm), as shown in Scheme 1A. The patterned mask of this paper-based microfluidic electrochemical immunodevice was designed in two dimensions using AutoCAD2012. Paper-A contains a central connecting zone (diameter = 7.0 mm) surrounded by eight working zones (diameter = 4.0 mm). Corresponding to paper-A, there is one circular connecting zone (diameter = 7.0 mm) in the center of paper-B. The fabrication procedure of this immunodevice is the following: Whatman chromatography paper #1 was impregnated with SU-8 3010 photoresist and then spin-coated at 2000 rpm for 30 s to spread the photoresist over the paper uniformly. The photoresist-coated paper was pre-baked on a hotplate at 95 °C for 10 min. The paper was tightly covered with a pre-designed film photomask and irradiated with a UV light (345 nm, 17 mW cm^{-2}) for 30 s. After post-baking at 95 °C for 1 min, the unpolymerized photoresist was chemically washed away by immersing the paper into acetone for 1 min and rinsing with acetone. Then, the paper was dried in a vacuum oven for 10 min and was ready to use. The region soaked by photoresist is impermeable to liquid, whereas the photoresist-eluted region remains hydrophilic.

Eight working electrode zones were screen-printed with carbon ink in a specific area on paper-A. Similarly, carbon ink and Ag/AgCl ink were screen-printed on a predesigned area of paper-B as the counter electrode and the reference electrode, respectively. Eight working electrodes share one pair of counter and reference electrodes after the two paper layers were stacked together.

2.4. Synthesis of initiator coupled signal antibody

The *N*-hydroxysuccinmidyl bromoisobutyrate (initiator) was prepared according to previous report (shown in Supporting information) (Lou et al., 2005). We synthesized four kinds of initiator-coupled signal antibody: initiator-coupled CEA signal antibody, initiator-coupled AFP signal antibody, initiator-coupled CA125 signal antibody and initiator-coupled CA153 signal antibody. The prepared NHS-coupled initiator (10 mg mL^{-1} in DMF, 10 μL) was added to a CEA, AFP, CA125 or CA153 signal antibody solution at 10 mg mL^{-1}, respectively, where the molar ratio of initiator to antibody was controlled at 8:1. The mixture was stirred overnight to allow the coupling reaction reaching completion and the excess NHS ester to hydrolyze. The concentration of the solution was determined by UV absorbance at 280 nm, and then diluted with PBS buffer (0.1 M, pH 7.4) to 1 mg mL^{-1}.

2.5. Preparation of paper-based microfluidic electrochemical immunodevice

Graphene oxide (GO) was synthesized from graphite through the modified Hummers method (Li and Wu, 2009; Liu et al., 2010). The as-synthesized graphite oxide was suspended in water and subjected to dialysis for one week to remove any residual salts. After drying at 50 °C overnight, the as-purified graphite oxide was exfoliated into GO by ultrasonicating a 0.05 wt% aqueous dispersion for 30 min. The unexfoliated graphite oxide was removed

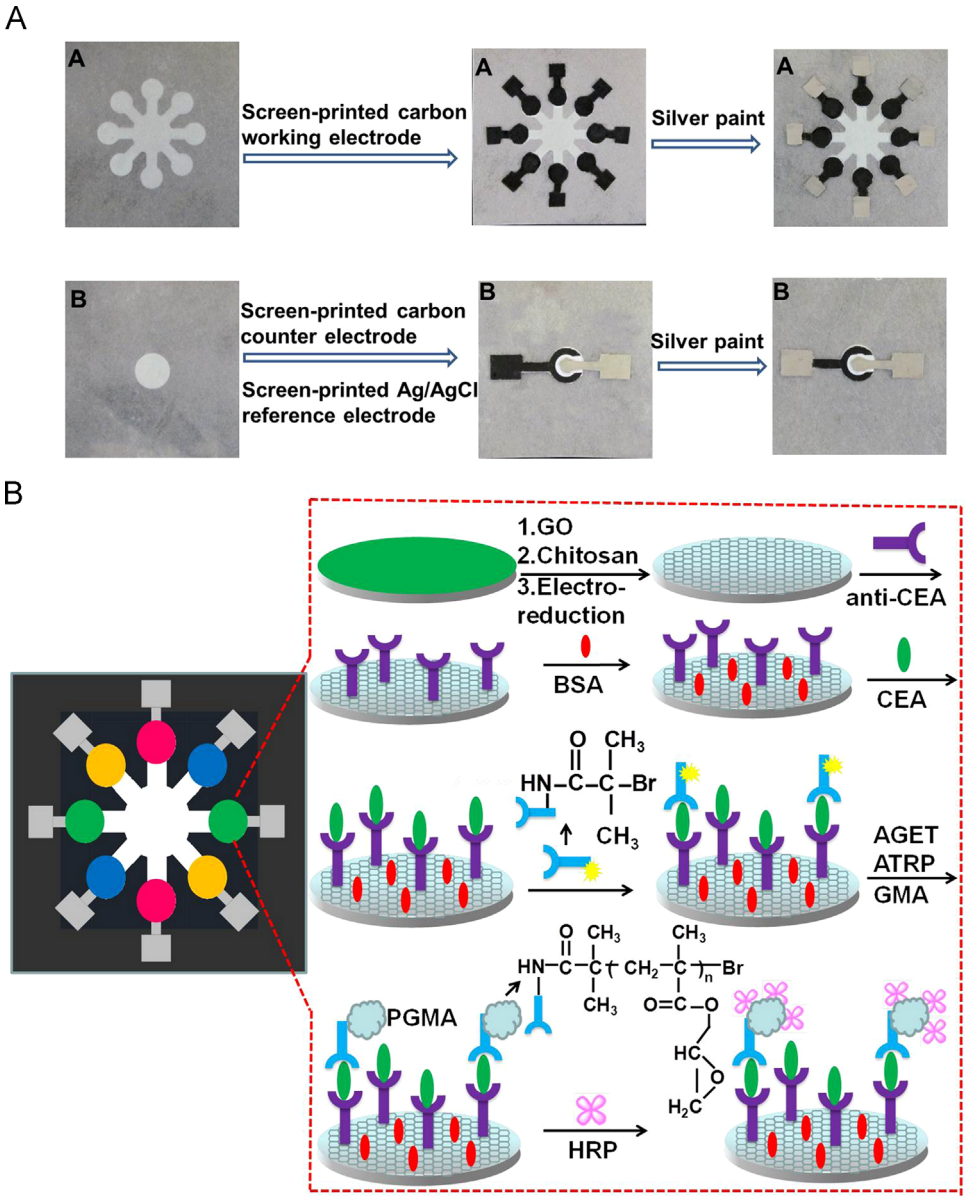

Scheme 1. (A) A photographed presentation on the fabrication process of the microfluidic paper-based electrochemical immunodevice. (B) Schematic representation of the fabrication and assay procedure used to prepare the paper-based microfluidic electrochemical immunodevice. CEA was provided as an example.

through a 5-min ultrafiltration at 2000 rcf. Then, 2 μL of 0.5 mg mL^{-1} GO solution was dropped onto each working electrode, and dried in air. Then, 2 μL of 0.05% chitosan solution was dropped onto the GO film and dried in air. After the electrochemical reduction of GO at −1.0 V in pH 7.4 PBS, the modified electrode was washed with water, incubated with 2 μL of 2.5% glutaraldehyde (in 50 mM PBS, pH 7.4) for 2 h, and washed with water. Then, 2 μL of 20 μg mL^{-1} CEA, AFP, CA125, and CA153 capture antibodies were applied to the corresponding working electrodes, and reacted at room temperature for 30 min. Subsequently, the excess antibodies were washed with pH 7.4 PBS containing 0.05% Tween-20. We then treated each working electrode by adding 2.0 μL of pH 7.4 PBS containing 0.5% BSA to block any possible remaining active sites against nonspecific adsorption and allowed the working electrodes to dry for 15 min under ambient conditions. After washing with pH 7.4 PBS containing 0.05% Tween-20, the resulting paper-based microfluidic electrochemical immunodevice was stored at 4 °C in a dry environment prior to use.

2.6. Electrochemical detection of cancer biomarkers

The electrochemical detection procedures are shown in Scheme 1B. To perform the immunoreactions and electrochemical detections, 2.0 μL of the sample solution containing different concentrations of CEA, AFP, CA125, and CA153 in PBS was added to each working electrode, allowed to incubate for 250 s at room temperature, and washed with pH 7.4 PBS containing 0.05% Tween-20. Then, 2.0 μL of 1 mg mL^{-1} initiator coupled signal CEA antibody, initiator coupled signal AFP antibody, initiator coupled signal CA125 antibody, and initiator coupled signal CA153 antibody were added to the corresponding working electrodes respectively and allowed to incubate for 250 s at room temperature. The polymerization was performed by immersing initiator modified immunodevice in a mixture of $CuCl_2$ (10 mg), bpy (23.45 mg), GMA (2 mL), DMF (1 mL), DI H_2O (1 mL) in a glass container. Then, 125 μL ascorbic acid was added to reduce Cu(II) ions and start the AGET ATRP reaction for 2 h. Following that, the immunodevice was thoroughly rinsed with acetone to remove

nonspecifically adsorbed monomers, then 2 μL 1 mg mL^{-1} HRP water solution was dropped onto each working electrode for 10 h at room temperature to bring HRP onto the immunodevice surface prior to electrochemical detection.

3. Results and discussion

3.1. Electrochemical and photometric assay of polymer growth atop initiator modified paper-based electrochemical immunodevice

GMA was the chosen monomer for AGET ATRP, which provided accessible side-chain functional groups that allow straightforward coupling of HRP. Initiator coupled signal antibody was immobilized on the working electrode surface through sandwich immunoreactions. The immunodevice was then immersed in an AGET ATRP reaction mixture containing GMA as the monomer, $CuCl_2$ and 2,2′-bipyridine (bpy) as the reaction catalyst. Also added in the reaction mixture was ascorbic acid, which served as the reducing agent to bring Cu(II) complexes back to the corresponding ATRP-active, lower oxidative state of catalytic Cu(I) complexes (Fig. 1A). A layer of PGMA film was formed on the working electrode surface after a 2 h reaction. Growth of the polymer materials provided numerous epoxy groups on the side chain of PGMA, which allowed the accumulation of electroactive molecule HRP on polymers through the reaction between the epoxy groups of polymers and the amino groups of HRP. Fig. 1B presents the DPV response of different electrodes in the presence of *O*-phenylenediamine and H_2O_2, CEA was used as an example. A DPV peak located at −0.548 V for the electrode where HRP was permanently anchored on the surface grafted with PGMA atop initiator coupled CEA signal antibody was clearly observed (curve a). To ensure the signal did not originate from nonspecific absorption of HRP, two control experiments were conducted. One of the control experiments had the concentration of CEA at 0 ng mL^{-1} (curve b), the other used CEA, without coupling of initiators, immobilized on electrode surface in a similar fashion (curve c). Much lower DPV responses for both electrodes were obtained, which suggested that the obvious DPV response in curve a can be attributed to the presence of HRP on the electrode surface and that the noise signal can be neglected. To verify the polymerization-assisted signal amplification, HRP directly labeled CEA signal antibody was used to complete the sandwich immunoreactions (curve d). The DPV signal was more than 2-fold lower than that of the electrode with the polymers. Therefore, this result confirmed the effect of the polymerization-assisted signal amplification. To verify the signal amplification of graphene, the CEA capture antibody was directly coupled to the electrode surface through chitosan, and a comparatively lower response was obtained (curve e), which indicates that the presence of graphene greatly increased the density of the CEA capture antibody on the electrode surface and further enhanced the overall signal detected.

The bound HRP on the electrode surface can also be determined by a photometric assay using tetramethyl benzidine (TMB) as the substrate (Liu et al., 2005). When the modified electrode was dipped into the TMB-H_2O_2 mixture solution, a large absorbance at 654 nm was observed (Supporting information, Fig. S1). The absorbance proportionally increased with the concentration of CEA in the incubation solution used for the preparation of the immunodevices, which ranged from 0.01 ng mL^{-1} to 100 ng mL^{-1}, with a correlation coefficient of 0.998. All of these results demonstrate that HRP was successfully coupled to the electrode surface and that our proposed signal-amplification strategy is feasible.

3.2. Characterization of the paper-based microfluidic electrochemical immunodevice

The electrochemical impedance spectroscopy (EIS) of the resulting paper working zones provides information on the successful assembly of the capture antibodies on the electrode surface. In this work, a $[Fe(CN)_6]^{3-/4-}$ redox couple was used to characterize the immunodevice features through electrochemistry. The original paper working zone on the immunodevice revealed a small semicircle domain (Fig. 2A, curve a), which implies a relatively low electron transfer resistance of the redox couple. After GO was assembled on the immunodevice, the resistance decreased (Fig. 2A, cure b) because the existence of the GO led to an increase in the electron transfer kinetics of $[Fe(CN)_6]^{3-/4-}$ and the effective conductive gap on the electrode/paper interface. It was observed that the chitosan-modified immunodevice exhibited a significantly lower resistance for the redox probe (Fig. 2A, curve c), which may be due to the electrostatic adsorption of the redox couple on the electrode substrate. More specifically, the working condition of this device is controlled at pH 7.4, under which the amino groups of chitosan should be protonated to positively charged $-NH_3^+$ groups (as the pKa is about 6.5). Thus the chitosan-modified surface can adsorb a significantly higher amount of $[Fe(CN)_6]^{3-/4-}$ anions than the bare substrate due to electrostatics, which creates a dense reservoir of redox couple at the electrode surface. Compared with the unbound $[Fe(CN)_6]^{3-/4-}$

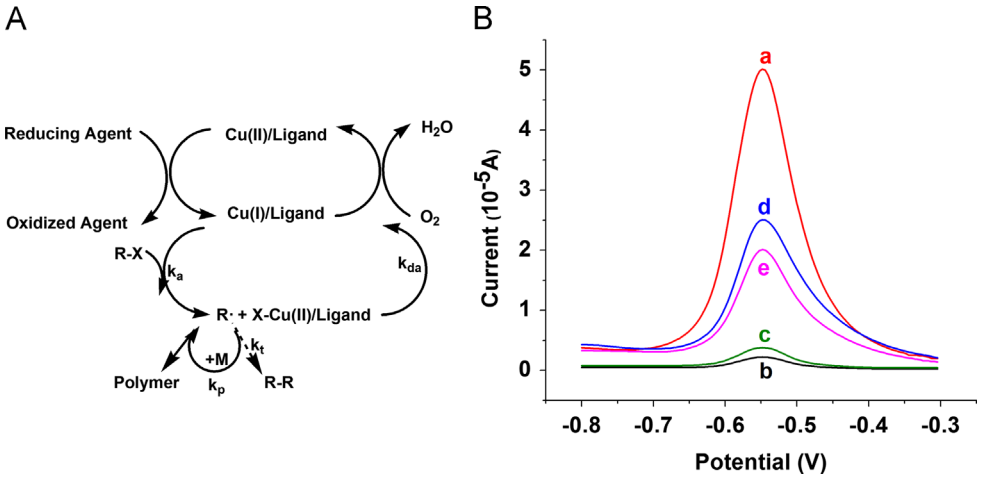

Fig. 1. (A) The mechanism of AGET ATRP; (B) DPV curves obtained from (a) HRP permanently anchored on the surface grafted with PGMA atop initiator coupled CEA signal antibody/CEA/anti-CEA/chitosan/electrochemically reduced GO/working electrode, (b) the concentration of CEA was 0 ng mL^{-1}; (c) CEA signal antibody without initiator; (d) HRP directly labeled anti-CEA was used as signal tags; and (e) GO was not used, other steps were the same with curve a.

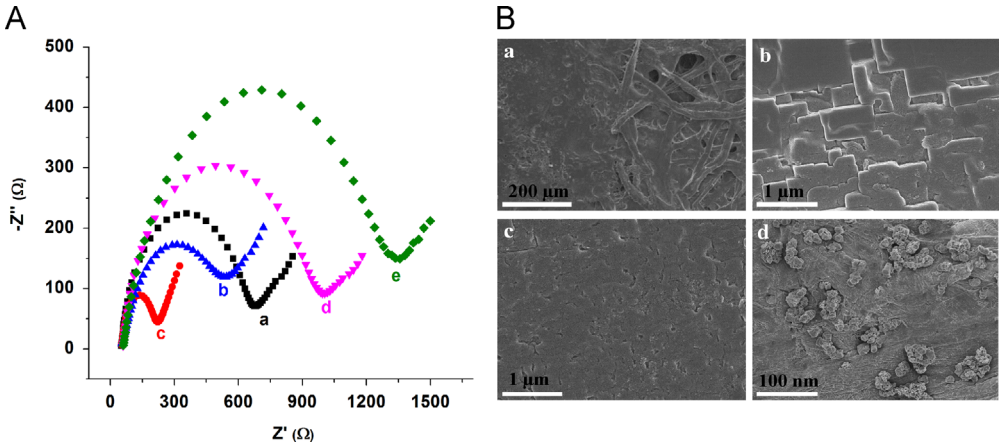

Fig. 2. (A) Electrochemical impedance spectroscopy (EIS) of (a) the original working electrode, (b) the GO/working electrode, (c) the chitosan/electrochemically reduced GO/working electrode (c), and the anti-CEA/glutaraldehyde/chitosan-modified working electrode (d) before and (e) after blocking with BSA in 0.1 M KCl containing 5.0 mM $[Fe(CN)_6]^{3-}$ and 5 mM $[Fe(CN)_6]^{4-}$. (B) SEM images of (a) the boundary of the photoresist pattern (left, photoresist soaked paper; right, pure paper), (b) GO/working electrode, (c) chitosan/electrochemically reduced GO/working electrode, (d) polymers formed on the working electrode.

anions alienated by the untreated substrate, the absorbed $[Fe(CN)_6]^{3-/4-}$ anions have much stronger interaction and electron-transfer ability with the electrode during redox reaction. Therefore, the chitosan-modified surface has a much lower charge transfer resistance for the redox probe of $[Fe(CN)_6]^{3-/4-}$. The similar phenomenon has been reported in literature (Zang et al., 2012). However, the diameter of the EIS curve obtained for the antibody-modified immunodevice, which was modified through glutaraldehyde linking, increased markedly (Fig. 2A, curve d) because the association of glutaraldehyde with chitosan obturated many amino groups of chitosan and formed a protein barrier for electron transfer. Similarly, BSA could also resist the electron-transfer kinetics of the redox probe at the paper interface, which resulted in an increased impedance of the paper working zone (Fig. 2A, curve e) and verified the immobilization of BSA.

SEM of the resulting paper working zones might provide further information on the assembly process. This immunodevice was fabricated on pure cellulose paper. The hydrophilic electrochemical cells were constructed through the selective polymerization and elution of the photoresist soaked in the paper fibers (Fig. 2B-a). Therefore, the liquid conduction was limited to the hydrophilic paper channels confined by the bulk region soaked with polymerized photoresist. After the GO was coated on the surface of the working zone, a structure of crumpled sheets was generated, as shown in the SEM image (Fig. 2B-b). The coating of chitosan on the electrochemically reduced GO film led to a smoother and more uniform surface topography (Fig. 2B-c). When the polymers were formed after 2 h of AGET ATRP, several polymer islands with an average diameter of approximately 20 nm were observed (Fig. 2B-d), which indicates the successful modification of the surface of the immunodevice after each step.

3.3. Optimization of the immunoassay conditions

AGET ATRP, a living polymerization reaction, which offers the benefit of tuning the length of polymer chains by varying the reaction time, i.e., a longer reaction time results in a higher amount of epoxy groups that are available for HRP coupling. Fig. 3A displayed the effect of polymerization time on DPV signal. The signal increases linearly as the polymer chain grows longer, however, the signal starts to level off after 2 h. This slow-down signal could be due to slow-down of polymer growth from radical termination, which reduced the accessibility of epoxy groups on the side chain of PGMA for HRP coupling or bigger steric hindrance. Thus the AGET ATRP time was fixed at 2 h throughout the study.

The amount of antigen captured from the solution depends on the incubation time before it reaches thermodynamic equilibrium. At room temperature, the DPV response increased with increasing incubation times in the sandwich-type immunoassays and then stabilized, which indicates the achievement of saturated binding in the immunoreaction (Fig. 3B). The optimal incubation time of CEA immunocomplexes was 250 s, and, accordingly, an incubation time of 250 s was selected for the subsequent experiments. The incubation process for this microfluidic paper-based electrochemical immunodevice comparatively required a much shorter incubation time than that required for traditional electrochemical immunoassays, which normally require 1–3 h of incubation at 37 °C. This difference is partly due to the high surface-to-volume ratio, the incompact porous structure, and the small volume of the graphene/chitosan-modified paper working zone. The immunoreagents need only to diffuse relatively short distances to the working electrodes to react with each other. Furthermore, as the solutions evaporate in the paper zones, the concentrations for each reagent increase, which may further enhance the binding kinetics and the formation of antibody–antigen immune complexes (Cheng et al., 2010). The short incubation time is an added advantage for development of ultrasensitive and high-throughput strategies.

The pH of the detection solution is another important factor in the enzymatic response. The effect of the solution pH on the DPV responses to CEA were investigated (Fig. 3C). The response increased as the pH value increased from 6 to 7.4 and then decreased at pH values higher than 7.4. Thus, the DPV detection was performed in pH 7.4 PBS.

3.4. Analytical performance

The analytical performance of this method was verified by applying 2.0 μL of samples of human CEA, AFP, CA125, and CA153 standard solutions at various concentrations in PBS under the optimized conditions. The DPV response and calibration curves for the four cancer biomarkers are shown in Fig. 4. With increasing concentrations of CEA, AFP, CA125, and CA153, good correlations between the concentration of the cancer biomarkers and the DPV response were observed with similar wide dynamic ranges (0.01–100 ng mL^{-1}, 0.01–100 ng mL^{-1}, 0.05–100 ng mL^{-1}, and 0.05–100 ng mL^{-1}, respectively), which corresponded to the levels that occur naturally in human blood plasma or serum. The linear regression equations were $I=2.47+1.02$ log $(C_{CEA}/ng\ mL^{-1})$ ($R^2=0.998$), $I=2.44+0.97$ log $(C_{AFP}/ng\ mL^{-1})$ ($R^2=0.996$), $I=2.12+1.02$ log $(C_{CA125}/ng\ mL^{-1})$ ($R^2=0.994$), and $I=1.95+1.04$ log $(C_{CA153}/ng\ mL^{-1})$ ($R^2=0.995$),

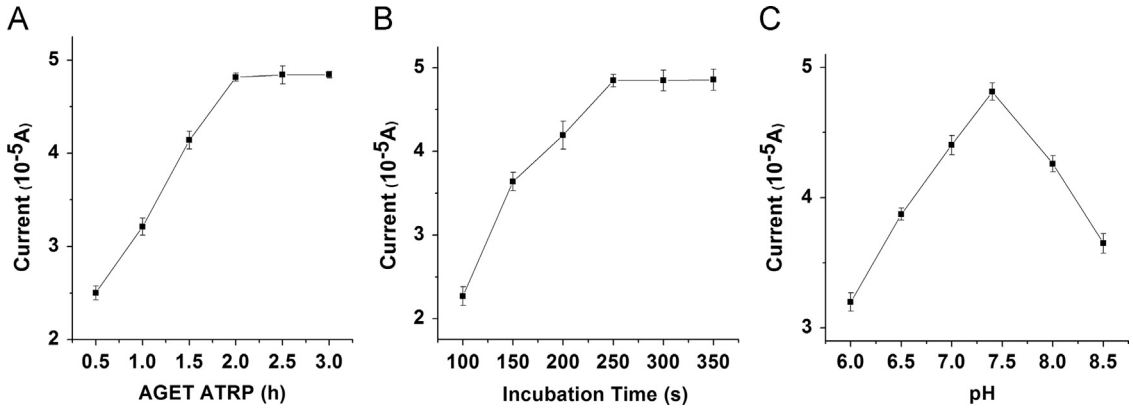

Fig. 3. Parameters affecting DPV signals in paper-based microfluidic electrochemical immunodevice. (A) Effect of AGET ATRP time on the DPV response. (B) Effect of the incubation time on the DPV response. (C) Effect of pH on the DPV response. 100 ng mL^{-1} CEA was used as an example.

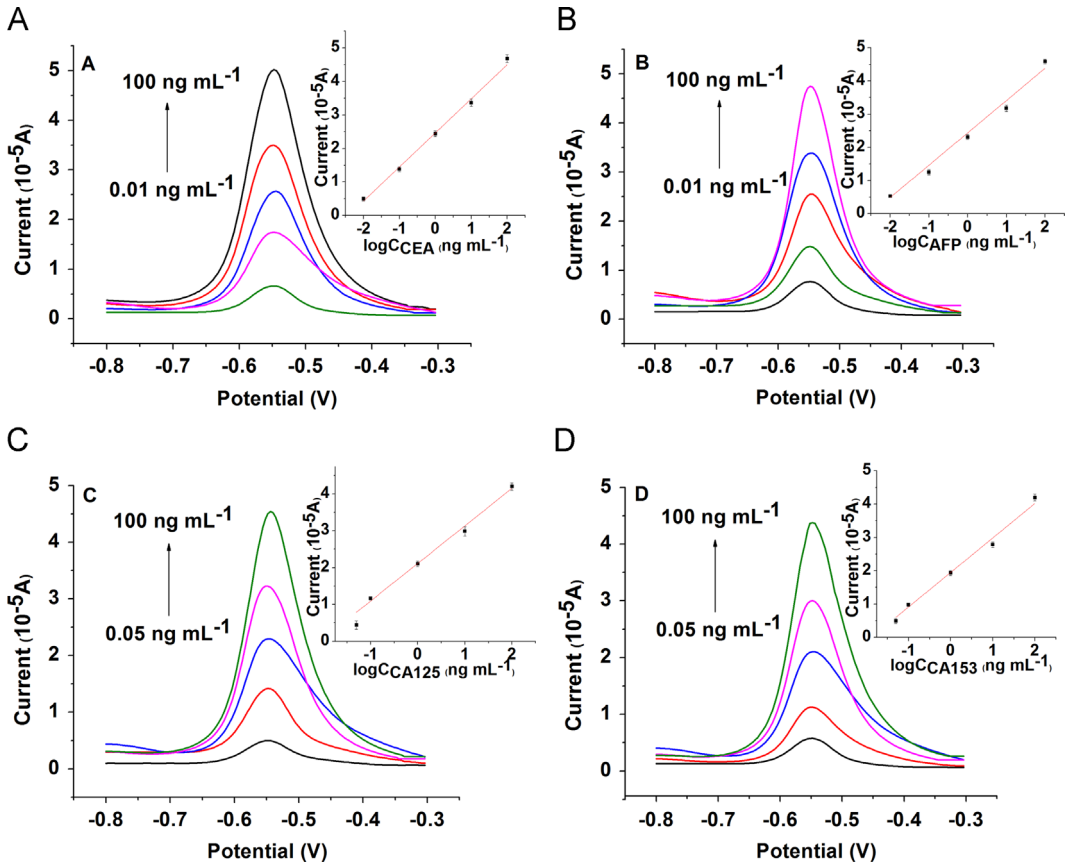

Fig. 4. Plots showing the DPV response with different concentrations of (A) CEA, (B) AFP, (C) CA125, and (D) CA153 in the incubation solutions. Inset: calibration curves for CEA, AFP, CA125, and CA153.

respectively, where *I* was the DPV response and *C* was the concentration of the cancer biomarker. The lowest detectable concentrations for the four cancer biomarkers were 0.01 ng mL^{-1}, 0.01 ng mL^{-1}, 0.05 ng mL^{-1}, and 0.05 ng mL^{-1}, respectively. These levels were lower than those reported in earlier studies (Wang et al., 2012a, 2012b; Ge et al., 2012a, 2012b).

3.5. *Evaluation of cross-talk on this paper-based microfluidic electrochemical immunodevice*

To confirm the resistance to cross-talk, the cross-reactivity between the analytes and non-cognate antibodies was investigated. In this paper-based microfluidic electrochemical immunodevice, four different capture antibodies for CEA, AFP, CA125 and CA153 were immobilized separately onto eight working electrodes. The cross-reactivity was evaluated by comparing the DPV responses obtained when the device was either incubated with a blank solution or 100 ng mL^{-1} of CEA, AFP, CA125, or CA153. As expected, only the working electrode prepared with the corresponding capture antibodies yielded obvious DPV responses (Fig. 5). The cross-reactivity detected between the analytes and non-cognate antibodies was also negligible. In addition, as shown in Fig. 1, the low nonspecific adsorption of the signal reporter with the working electrodes further indicated that the potential cross-talk between the electrodes is negligible in this microfluidic paper-based electrochemical immunodevice. Therefore, it is feasible to perform simultaneous multianalyte

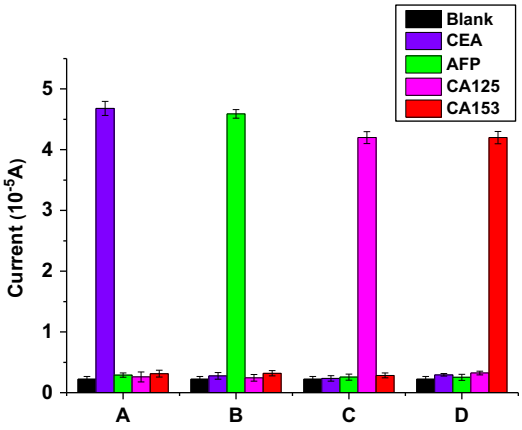

Fig. 5. The cross-reactivity between the working electrodes was negligible. DPV response detected for the different antigens on the different electrodes: (A) anti-CEA/chitosan/electrochemically reduced GO/working electrode, (B) anti-AFP/chitosan/electrochemically reduced GO/working electrode, (C) anti-CA125/chitosan/electrochemically reduced GO/working electrode, and (D) anti-CA153/chitosan/electrochemically reduced GO/working electrode.

immunoassays with this disposable paper-based microfluidic electrochemical immunodevice.

3.6. Reproducibility, precision, stability, and regeneration of immunodevice

Both the intra-assay and inter-assay precision of the immunodevice were evaluated by assaying CEA levels with 100 ng mL^{-1} through five replicate measurements in the same run (for determination of the intra-assay precision) and in different runs (for determination of the inter-assay precision). The relative standard deviations (RSD) were 6.3% and 7.8%, respectively, which indicate that the device exhibits good precision and fabrication reproducibility. In addition, we also stored the dry immunodevice at 4 °C (sealed) and subsequently employed it for immunoassays at intervals of 3 days. No obvious change in the performance could be observed after the device was stored for up to 3 weeks. These results indicate that the immunodevice exhibits acceptable reliability and stability.

Lastly, the regeneration of the immunodevice was achieved by incubating it with 0.1 M glycine–HCl (pH 2.2) to dissociate the antigen–antibody complexes. Using the regeneration procedures, the paper-based microfluidic electrochemical immunodevice could be recycled at least 25 times without any obvious loss in its analytical performance.

4. Conclusion

In summary, we have demonstrated here that a controlled radical polymerization reaction, AGET ATRP, can be introduced into a simple paper-based microfluidic electrochemical immunodevice for the ultra-sensitive and high-throughput detection of cancer biomarkers. The surface in situ polymerization provided numerous epoxy groups on the side chain of PGMA for local accumulation of electrochemically active probes. The introduction of graphene onto the surface of the immunodevice efficiently accelerated the electron transfer and further enhanced the detection signal. The immunodevice proposed in this work combined the simplicity and low cost of paper-based microfluidic immunodevices with the ultra-sensitivity of signal amplification strategies. In addition to the clinical applications for the detection of cancer biomarkers, the immunodevice described in this paper could also be easily adapted for the identification of other soluble compounds, such as enzymes and nucleic acids. Thanks to the fast development of modern electronics, many current manufacturers have been able to integrate the powerful electro-analysis functions into an extremely compact and handheld potentiostat/galvanostat system, such as PG581 by Uniscan Instruments, PocketSTAT by Ivium Technologies, and 1200B by CH Instruments. Combined with these state-of-the-art handheld instruments commercially available, our paper device can enable rapid, low-cost, disposable and yet recyclable, and portable point-of-care diagnostics, which could significantly benefit the healthcare in the resource-poor settings.

Acknowledgements

This work was supported by a start-up grant from Nanyang Technological University College of Engineering, an Academic Research Fund Tier-1 from the Ministry of Education of Singapore (RG 26/11) awarded to Y.K., and research grants from the SingHealth Foundation, the Singapore National Medical Research Council, the Biomedical Research Council of Singapore, and the Singapore Millennium Foundation awarded to K.M.H.

Appendix A. Supplementary material

Supplementary data associated with this article can be found in the online version at http://dx.doi.org/10.1016/j.bios.2013.08.039.

References

Abe, K., Suzuki, K., Citterio, D., 2008. Analytical Chemistry 80, 6928–6934.
Apilux, A., Dungchai, W., Siangproh, W., Praphairaksit, N., Henry, C.S., Chailapakul, O., 2010. Analytical Chemistry 82, 1727–1732.
Bruzewicz, D.A., Reches, M., Whitesides, G.M., 2008. Analytical Chemistry 80, 3387–3392.
Cheng, C.M., Martinez, A.W., Gong, J., Mace, C.R., Phillips, S.T., Carrilho, E., Mirica, K.A., Whitesides, G.M., 2010. Angewandte Chemie International Edition 49, 4771–4774.
Coll, C., Bernardos, A., Martinez-Manez, R., Sancenon, F., 2013. Accounts of Chemical Research 46, 339–349.
Fu, B., Cao, J.C., Jiang, W., Wang, L., 2013. Biosensors and Bioelectronics 44, 52–56.
Ge, L., Wang, S.M., Song, X.R., Ge, S.G., Yu, J.H., 2012a. Lab on a Chip 12, 3150–3158.
Ge, L., Yan, J.X., Song, X.R., Yan, M., Ge, S.G., Yu, J.H., 2012b. Biomaterials 33, 1024–1031.
Geissler, D., Stufler, S., Lohmannsroben, H.G., Hildebrandt, N., 2012. Journal of the American Chemical Society 135, 1102–1109.
Karra, S., Zhang, M.G., Gorski, W., 2013. Analytical Chemistry 85, 1208–1214.
Lei, J.P., Ju, H.X., 2012. Chemical Society Reviews 41, 2122–2134.
Li, Y.G., Wu, Y.Y., 2009. Journal of the American Chemical Society 131, 5851–5857.
Liu, J.B., Fu, S.H., Yuan, B., Li, Y.L., Deng, Z.X., 2010. Journal of the American Chemical Society 132, 7279–7281.
Liu, S.Q., Wollenberger, U., Halamek, J., Leupold, E., Stocklein, W., Warsinke, A., Scheller, F.W., 2005. Chemistry—A European Journal 11, 4239–4246.
Lou, X.H., He, L., 2006. Langmuir 22, 2640–2646.
Lou, X.H., Lewis, M.S., Gorman, C.B., He, L., 2005. Analytical Chemistry 77, 4698–4705.
Lu, Y., Shi, W., Qin, J., Lin, B., 2009. Analytical Chemistry 82, 329–335.
Martinez, A.W., Phillips, S.T., Butte, M.J., Whitesides, G.M., 2007. Angewandte Chemie International Edition 46, 1318–1320.
Martinez, A.W., Phillips, S.T., Wiley, B.J., Gupta, M., Whitesides, G.M., 2008. Lab on a Chip 8, 2146–2150.
Martinez, A.W., Phillips, S.T, Whitesides, G.M., 2010. Analytical Chemistry 82, 3–10.
Mentele, M.M., Cunningham, J., Koehler, K., Volckens, J., Henry, C.S., 2012. Analytical Chemistry 84, 4474–4480.
Noh, H., Phillips, S.T., 2010. Analytical Chemistry 82, 8071–8078.
Olkkonen, J., Lehtinen, K., Erho, T., 2010. Analytical Chemistry 82, 10246–10250.
Qian, H., He, L., 2009a. Analytical Chemistry 81, 4536–4542.
Qian, H., He, L., 2009b. Analytical Chemistry 81, 9824–9827.
Schilling, K.M., Lepore, A.L., Kurian, J.A., Martinez, A.W., 2012. Analytical Chemistry 84, 3484.
Sia, S.K., Kricka, L.J., 2008a. Lab on a Chip 8, 1988–1991.
Sia, S.K., Kricka, L.J., 2008b. Lab on a Chip 8, 1982–1983.
Wang, P.P., Ge, L., Yan, M., Song, X.R., Ge, S.G., Yu, J.H., 2012a. Biosensors and Bioelectronics 32, 238–243.
Wang, P.P., Ge, L., Ge, S.G., Yu, J.H., Yan, M., Huang, J.D., 2013. Chemical Communications 49, 3294–3296.

Wang, S.M., Ge, L., Song, X.R., Yu, J.H., Ge, S.G., Huang, J.D., Zeng, F., 2012b. Biosensors and Bioelectronics 31, 212–218.
Whitesides, G.M., 2011. Lab on a Chip 11, 191–193.
Wu, Y.F., Liu, S.Q., He, L., 2009. Analytical Chemistry 81, 7015–7021.
Wu, Y.F., Shi, H.Y., Yuan, L., Liu, S.Q., 2010. Chemical Communications 46, 7763–7765.
Wu, Y.F., Liu, S.Q., He, L., 2011. Analyst 136, 2558–2563.
Xu, J., Wu, J., Zong, C., Ju, H.X., Yan, F., 2013. Analytical Chemistry 85, 3374–3379.
Yu, J.H., Wang, S.M., Ge, L., Ge, S.G., 2011. Biosensors and Bioelectronics 26, 3284–3289.
Zang, D., Ge, L., Yan, M., Song, X., Yu, J., 2012. Chemical Communications 48, 4683–4685.